

## Power System Stability by Improved Grasshopper Optimization Algorithm-Based PSS with Type-2 Fuzzy Lead-Lag based SSSC Controller

Sanat Kumar Patra<sup>1</sup> and Sangram Keshori Mohapatra<sup>2,\*</sup>

<sup>1</sup>Department of Electrical Engineering, Seemanta Engineering College, Mayurbhanj, Odisha, India

<sup>2</sup>Department of Electrical Engineering, Government College of Engineering, Keonjhar, Odisha, India

Received 19 July 2023; Accepted 31 October 2023

### Abstract

This article attempted coordinated control of Type-2 fuzzy PSS with type-2 fuzzy lead lag (T2FLL) based SSSC controller for enhancement of transient stability of the power system. The initial step of analysis a single machine infinite bus power system model with LL based SSSC controller and PSS is considered. It is formulated by optimization problem to find out the optimal controller parameters by employing improved Grasshopper Optimization Algorithm (iGOA), GOA, PSO and Genetic algorithm (GA). The proposed test model of Type-2 fuzzy PSS with T2FLL based SSSC controller over PSS with LL controller of the same power system model demonstrated under different fault condition and location of fault with change of loading condition. The second part of analysis to check the effectiveness and robustness of transient stability in multi machine power system (MMPS) uses Type-2 fuzzy PSS with T2FLL based SSSC controller. The proposed MMPS with Type-2 fuzzy PSS with T2FLL controller demonstrated and observed that it gives the better performances of damping of oscillation as compared to PSS with LL based SSSC controller under different fault condition of the power system.

**Keywords:** Power system stability, Static synchronous series compensator, Power system stabilizer, Type-2 fuzzy LL controller, Grasshopper optimization algorithm

### 1. Introduction

The weak tie lines connecting large power networks due to a disturbance it results in the formation of low frequency oscillations. In such cases, insufficient system damping may cause continuous oscillations of the system which in turn may cause separation of the system [1,2]. The Power system stabilizers (PSS) are often chosen by utilities as a solution to this problem. Since PSSs might not provide enough damping therefor the additional controllers are required. Due to recent developments in power electronics, it is now increases the essential to use flexible AC transmission system (FACTS) devices to resolve various problems in the power system. These devices' uses can improve the stability of power systems in a variety of situations due to their fast control capabilities of interconnection of power system. The SSSC is a member of the FACTS family which can regulate power flow in power systems by switching from capacitive to inductive mode. The SSSC controller is chosen in the suggested analysis to design of the power system since it supplied additional damping of the power system [3]. The various types of artificial intelligence (AI) computing-based strategies have been studied in the different power system damping controller design in the power system. In this studies some AI based approaches that have been analyzed in the proposed research such as Tabu Search (TS) [4], genetic algorithm (GA) [5,6], oppositional cuckoo algorithms (OCA)[7], simulated annealing (SA)[8], bacterial foraging algorithm (BFA)[9] and particle swarm optimization (PSO)[10]. Ant colony [11], Differential Evolution [12], chaotic krill herd blended runner root algorithm [13], hybrid

shuffled frog-leaping & pattern search (hSFLA-PS) technique [14]. The coordination control in PSS with FACTS based damping controller design has been studied in different power systems. As per the literature studies, coordinated control of PSS with SSSC employed PSO [15], PSS with ant colony optimization algorithm [16], PSS with SSSC-POD controller employed Mayfly algorithm [17], PSS with SSSC controller used hybrid whale & nelder mead approach [18], PSS with STATCOM by Self-Adaptive Learning Bat Algorithm (SALBA)[19], PSS with FACTS based GOA[20] optimization techniques has been attempted for the improvement of stability of the power system.

The majority cases in the literature studies shows that the application of power system stability analysis the lead-lag (LL) based controllers has been attempted in the different power system. The researchers have recently suggested fuzzy logic-based controllers (FLC) as it has the ability to work with inaccurate inputs and capacity to operate nonlinearity. The improved control strategy in hybrid power system has been employed fuzzy PID regulator in the power system [21]. A UPFC damping controller and a PSS have been employed in combined to develop a FLC-based method described to suppress the power oscillation damping of the system [22]. It has been used to a hybrid fuzzy-neural approach for obtaining the optimum hybrid power generation of the system [23]. A mixture of firefly swarm optimized algorithm in type-2 fraction order fuzzy based PID controller with power system stabilizer has been attempted to improve the power system stability [24]. The robust interval type-2 fuzzy lead-lag employed Harris Hawks studies for power system stability improvement [25], adaptive fuzzy lead-lag used modified grasshopper in PSS with FACTS based controller for improvement of power system stability [26].

\*E-mail address: sangram.muna.76@gmail.com

ISSN: 1791-2377 © 2023 School of Science, IJU. All rights reserved.

doi:10.25103/jestr.166.03

As per the literature studies that different researches have been attempted various optimization techniques in different type of power system problem. There is no any optimization technique best suitable for all type of problems. There are various prospects for power system stability improvement performance which provided new and improvement type of optimization algorithm. Saremi et al. have developed an optimization technique which is inspired by nature and the social interactions of grasshoppers. This nature-inspired technique is called the Grasshopper Optimization Algorithm (GOA) [27,28]. It has been employed to solve numerous optimization problems as this technique is simplicity, ability to avoid high local optimum values, and gradient-free method. According to [27], the GOA approach is greatly outperformed by a number of optimization techniques such as GA, PSO, state of matter search (SMS), firefly algorithm (FA), flower pollination algorithm (FPA) and GSA. The GOA approach has been used to pick features for maximum classification performance which comparing the results of GOA to those of other feature selection methods including GA and PSO [29]. The GOA optimization algorithm has been attempted in optimal sizing of an autonomous microgrid system and the outcomes are compared to those of Cuckoo Search and PSO techniques [30]. For the global optimization of test functions, a chaotic GOA has been anticipated in [31], and it is shown that chaotic maps significantly improve GOA accuracy. The article [32] presents an exhaustive analysis of GOA and its variant are discussed. The two stages of the meta heuristic optimization process are commonly referred such as exploration and exploitation stage. The exploration is concerned with the potential of the algorithm to behave in a highly randomized manner in order to significantly alter the results. The presence of wide variances in the solutions encourages further investigation in the search space and the identification of parameters in attractive regions. The algorithms usually make advantage that it tendency to the solutions of regularly encounter smaller-scale variables and try to explore locally. The balancing between exploration and exploitation stage the search for the global optimum of a particular optimization problem can be accelerated. The concert of the actual GOA significantly depends on the coefficient of 'c' which is used to define the zones of attraction, repulsion, and comfort. The parameters of GOA gradually reduced from 1 to 0.00001. The modified to improve of GOA called iGOA optimization algorithm is employed in anticipated of this research work. In this iGOA optimization algorithm the coefficient 'c' is adjusted such a way that enhances algorithm performance. This paper suggested a iGOA optimized in coordinated control of type-2 fuzzy PSS with T2FLL based SSSC controller for enhancement of power oscillation damping of the power system. The novel contributions of the paper are

- i. To design of iGOA optimized based Type-2 fuzzy PSS with T2FLL based SSSC damping controllers suggested for power system stability improvement in the power systems.
- ii. Projected iGOA algorithm is first tested coordinated control of PSS with lead lag based SSSC controller compared to GOA, PSO, and GA optimal coordinated control of same power system to shows its superiority.
- iii. To demonstrated the Type-2Fuzzy PSS with T2FLL SSSC based controller superior over conventional PSS with LL controller under different loading and location of fault in SMIB power system.

- iv. The effectiveness and robustness analysis is demonstrated by extending multi machine two area power system.

## 2. System Under Investigation

### 2.1 Single Machine Infinite Bus

The SMIB power system as in Fig.1 is chosen initially. This SMIB system having the synchronous generator terminal voltage  $V_T$  and the infinite bus voltage  $V_B$  are considered. The T represents the transformer.  $V_1$  and  $V_2$  are used to denote the voltages on buses 1 and 2 respectively. The converter's output voltage is designated as  $V_{cnv}$  and the DC source voltage is denoted as  $V_{DC}$ . The PL and I represents the real power and current of the transmission line that connects buses 1 and 2. In contrast, PL1 stands for the real power that is transmitted along one of the two parallel lines. The synchronous generator which included a turbine, governor, field excitation and also incorporates the power system stabilizer. The Automatic Voltage Regulator (AVR) and exciter are components of the excitation system [33].

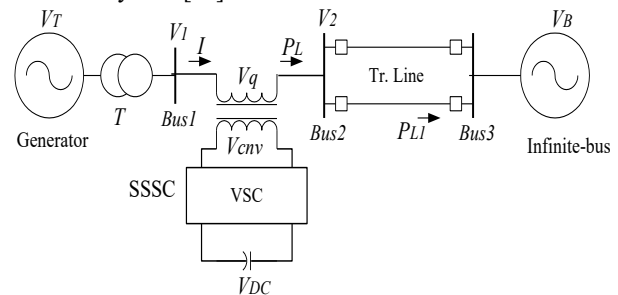


Fig. 1. Test model of SMIB power system

### 2.2 Kundur's Four Machine Two Area Test Power System

The Figure 2 shows the Kundur's four machine test system in which it consisting of 11 bus and two absolutely symmetrical areas combined through two parallel transmission lines of 220 km long distance. The Bus 7 and 9 are considered to have loads and shunt capacitors respectively. The low frequency oscillation was precisely planned in the power system as in reference [33]. The test system simulates features of typical systems that are used in actual operations. The constant impedances loads are used in the load of the proposed power system. The 413 megawatt of power is transferred from area-1 to area-2. Any disturbance of the power system under stress and causes it to oscillate. The system specifications are described in [33].

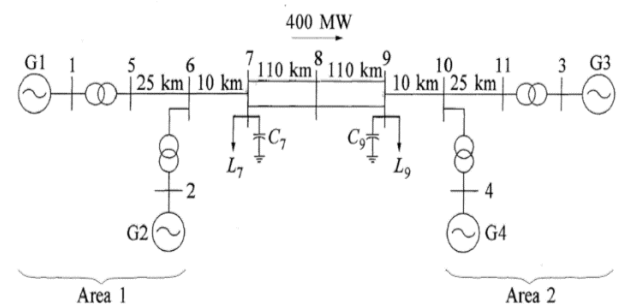


Fig. 2. Kundur's four machine test system

## 3. The Proposed Method

### 3.1 Outline of Type-2 Fuzzy Logic Control

The performance of a system may not be improved by using traditional fuzzy logic control (FLC) when there are significant uncertainties. The PSSs performance is enhanced using the type-2 double MF based controller. The proposed structure of the present work is a T2FLL controller considered for improvement of low frequency oscillation of damping of power system. The MFs of the type-2 FLC are uses by upper MF(UMF) and lower MF(LMF). A barrier is formed by combining the UMF and LMF. The construction of a foot print of uncertainty (FOU) is restricted between the UMF and LMF. A type-2 fuzzy operation contains defuzzification, knowledge base, type reducer and fuzzification. The fuzzification is first stage of fuzzy logic control system. It uses MFs to process inputs and provide the necessary structured fuzzy sets. The linguistic variables ‘EX\_N’, ‘L\_N’, ‘ZE\_R’, ‘L\_P’ and ‘EX\_P’ are employed as MFs to represent Extreme Negative, Least Negative, Zero, Least Positive and Extreme Positive respectively. The type-2 fuzzy set (FS) may be expressed as:

$$FS = ((Var, a), \mu_U(Var, a)), vVar \in P, va \in J_{Var}[0,1] \quad (1)$$

Where,

$\mu_U(Var, a)$  is the UMF,  $Var$  is the main variable,  $a$  is the added variable of domain  $J_{Var}$

The universe of discourse is expressed as:

$$FS = \int_{Var \in P} \int_{a \in J_{Var}[0,1]} \frac{\mu_E(Var, a)}{(Var, a)} \quad (2)$$

Where,  $\int$  = Union on ACE and  $a$

Now the equations can be written as:

$$\mu_{\bar{U}}(Var, a) = \overline{FOU(U)} vVar \in P, va \in J_{Var}[0,1] \quad (3)$$

Where,

$J_{Var}$  is expressed as:

$$J_{Var} = [\mu_{\bar{U}}(Var, a), \mu_U(Var, a)] vVar \in P, va \in J_{Var}[0,1] \quad (4)$$

The MF related to type-I FLC motivates to cultivate LMF and UMF. The knowledge base includes rule base and interface engine. The rule base is demonstrated in Table 1. Individually  $Var$  and  $dVar$  are the input signals to type-2 FLC which generates output  $y$ . The characteristic of the type-2 FLC is

$$LMF: forVar = \underline{LN}; dVar = \underline{Z}; Y = \underline{LN} \quad (5)$$

$$UMF: forVar = \overline{LN}; dVar = \overline{Z}; Y = \overline{LN} \quad (6)$$

The Type-2 fuzzy set firing forte is

$$\underline{f}^s = \min(\mu_{\bar{U}S}(Var, a), \mu_{\bar{U}S}(dVar, a)) \quad (7)$$

$$\overline{f}^s = \max(\mu_{\bar{U}S}(Var, a), \mu_{\bar{U}S}(dVar, a)) \quad (8)$$

$$F^s = [\underline{f}^s, \overline{f}^s] \quad (9)$$

Type-2 FS is transformed into type-1 FS using TR for defuzzification. Center of Sums, Centroid, and Center of Sets (SOC) are three defuzzification techniques, with SOC being considered the best.

It has the following results.:

$$Y_{cos} = \sum_{s=1}^{25} \frac{F^s y^s}{F^s} = [Y_{m1}, Y_{m2}] \quad (10)$$

$$Y_{m1} = \frac{\sum_{s=1}^{25} f^s y^s}{\sum_{s=1}^{25} \bar{f}^s y^s} \quad (11)$$

$$Y_{m1} = \frac{\sum_{s=1}^{25} f^s y^s}{\sum_{s=1}^{25} \bar{f}^s y^s} \quad (12)$$

where MFs of type-1 FLC are linked to  $Y_{m1}$  and  $Y_{m2}$ . Averaging is used to determine type-2 FLC's output All of the properties of lead lag controller and type-2 FLC are taken into consideration while arranging the proposed T2FLL.

**Table 1.** Demonstrated rule base Type-2 FLC

$\begin{matrix} \dot{e} \\ e \end{matrix}$	EX_N	L_N	ZE_R	L_P	EX_P
EX_N	EX_N	EX_N	L_N	L_N	ZE_R
L_N	EX_N	L_N	EX_N	ZE_R	L_P
ZE_R	L_N	L_N	ZE_R	L_P	L_P
L_P	L_N	ZE_R	L_P	L_P	EX_P
EX_P	ZE_R	L_P	L_P	EX_P	EX_P

### 3.2 Configuration of T2FLL Controller and Type-2 Fuzzy PSS

The Figure-3 illustrates the design of T2FLL based SSSC damping controller of the power system. The structure is made up of a sensor block, two lead lag blocks, a delay block, a gain block, and a washout block. It is usual to assume that the washout time constant is 10 seconds [33,35]. The appropriate phase-lead is delivered by the LL blocks to compensate for the delay between the input and output signals. The speed variations also chosen as the T2FLL controller input signal. The T2FLL controller assumes a transport delay of 50 ms and sensor time constant 15ms [10]. The Type-2 FLC based PSS consist of gain, sensor, washout, and two stage lead lag compensation block which as shown in Fig.4.

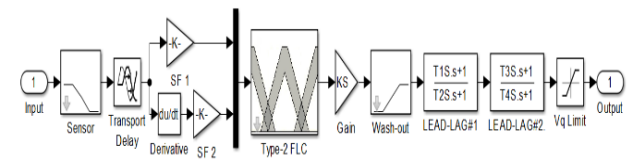


**Fig. 3.** T2FLL based SSSC controller

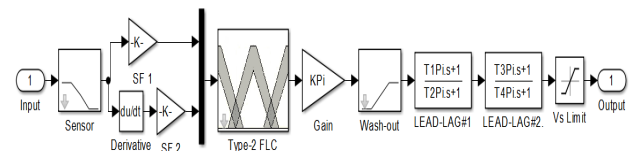


**Fig. 4.** Structure of Type-2 fuzzy PSS

The speed deviation taken as an input signal to the Type-2 fuzzy based PSS. The excitation voltage is adjusted using the PSS output ( $V_s$ ). The sensor is expected to have a 15 ms time constant.

**3.3 Optimization Problem:** The performance indices Integral Time Absolute value of Error (ITAE) is chosen as

objective function of SMIB power system. Similarly, MMPS the objective function chosen with speed deviation in local and inter area mode of oscillation. The ITAE value chosen in Equ.(13) & Equ.(14) for SMIB and MMPS must be minimized to improve the system transient performances of the system.

The objective function for SMIB is:

$$J = \int_{t=0}^{t=t_{sim}} |\Delta\omega| \cdot t \cdot dt \quad (13)$$

Where  $t_{sim}$  is the simulation duration and  $\Delta\omega$  is the deviation in rotor speed.

The objective function for MMPS is:

$$J = \int_{t=0}^{t=t_{sim}} (\sum |\Delta\omega_L| + \sum |\Delta\omega_I|) \cdot t \cdot dt \quad (14)$$

Where  $\Delta\omega_L$  and  $\Delta\omega_I$  are the speed variation corresponding to local and inter-area oscillation modes respectively. As a result, the optimization problem that represents the design problem which is as follows:

$$\text{Minimize } J \quad (15)$$

Subject to

$$\begin{aligned} K_{SF1mi} \leq K_{SF1} \leq K_{SF1max}, K_{SF2mi} \leq K_{SF2} \leq K_{SF2max} \quad K_{min} \leq K \\ \leq K_{max} \quad T_{1min} \leq T_1 \leq T_{1max}, T_{2min} \leq T_2 \leq T_{2max}, T_{3min} \leq T_3 \\ \leq T_{3max}, T_{4min} \leq T_4 \leq T_{4max} \end{aligned} \quad (16)$$

Where  $K_{SF1}$  and  $K_{SF2}$  are the scaling factors,  $K$  gains and  $T_1, T_2, T_3, T_4$  are the time constant. The range of the parameters for  $K$ , Time constants  $T_1, T_2, T_3, T_4$  and  $K_{SF}$  are [0.01 to 100], [0.01 to 10] and [0.01 to 100] respectively. The iGOA optimization algorithm is used in the present work to find out the tuning coordinated controller parameters of Type-2 Fuzzy PSS and T2FLL SSSC controller of the power system.

#### 4. Overview of GOA Optimization Algorithm and Its Improvement

Grasshopper optimization algorithm (GOA) is a nature-inspired optimization technique of social activities of grasshopper which is recently developed by, Saremi *et al.* [27]. At the time of seeking food, grasshopper exhibit swarming behaviour and transmits its act of searching abruptly and move locally for achieving its target. Such behaviours of grasshopper swarm are known as exploration and exploitation tendencies. Thus, for the designing of nature inspired algorithm for a mathematical model of grasshopper's behaviour. Therefore, the mathematical model used to simulate the swarming behaviour of grasshoppers is as follows

$$X_i = S_i + F_i + W_i \quad (17)$$

Where,  $X_i = i^{th}$  grasshopper's position,  $S_i =$  social interaction,  $F_i =$  force of gravity of  $i^{th}$  grasshopper,  $W_i =$  wind advection.

The random behaviour can be provided by reforming the above equation as  $X_i = r_1 I_i + r_2 F_i + r_3 W_i$

Where random numbers  $r_1, r_2$  and  $r_3$  in the interval [0, 1].

$$S_i = \sum_{\substack{l=1 \\ l \neq k}}^N s(d_{kl}) \cdot \hat{d}_{kl} \quad (18)$$

Where,  $d_{kl} = |X_l - X_k|$  = represent the grasshopper distance between  $k^{th}$  and  $l^{th}$  and  $\hat{d}_{kl} = \frac{X_l - X_k}{d_{kl}}$  is represent as  $k^{th}$  to  $l^{th}$  grasshopper of unit vector.

The function  $s$  is defined as social forces which shows the influence on the social interaction of grasshopper and this force can be calculated as follow

$$s(r) = ae^{-\frac{r}{l}} - e^{-r} \quad (19)$$

Where, ' $l$ ' indicates the attractive length scale and ' $a$ ' indicates the intensity of attraction.

It is seen that as per suggested the function  $s$  is taken within 0 and 15 [29], then repulsion take place in the interval [0 2.079] and attraction increases from 2.079 to 4-unit distance which decreases gradually. It is also suggested that there exist no interactive forces while two grasshoppers are 2.079 units apart from each other. This distance is known as comfortable distance and the corresponding zone is known as the comfortable zone. It is evident from equation-(19) that, there is a variation of parameters ( $l$  &  $a$ ) causes significant changes in attraction, repulsion and comfort zones causing social behaviors of artificial grasshoppers. The function ' $s$ ' is the social force that can separate space among two grasshoppers into attraction, repulsion and comfort zone. However if the distance is more than 10, the function ' $s$ ' returns value near to zero and become incapable to apply forces among grasshoppers due to the large distance between the grasshoppers. The separation between grasshoppers in the range taken as [1, 4] for determining the above problem. From Eq.(17), the  $F$  component can be calculated as

$$F_i = -g\hat{e}_g \quad (20)$$

where,  $g$  represents the gravitational constant and  $\hat{e}_g$  represents a unit vector towards the center of the earth.

From Eq.17, the component  $W$  is calculated as

$$W_i = u\hat{e}_w \quad (21)$$

where  $\hat{e}_w$  is the unity vector in the wind direction and  $u$  represents drift constant

As Nymph grasshoppers have no wings, their movements are more interrelated with the wind direction. Considering number of grasshoppers equals to 'N' and putting the expressions of SF and  $W$  in Eq. (19), it can be developed as

$$X_i = \sum_{\substack{l=1 \\ l \neq k}}^N s(|X_l - X_k|) \frac{X_l - X_k}{d_{kl}} - g\hat{e}_g + u\hat{e}_w \quad (22)$$

Nymph grasshoppers have no wings and they land on the ground and their positions must not be taken less than the threshold value. Thus Eq. (22) can be used for simulation of nature of interaction among grasshoppers in a swarm. Keeping in view of the fact that, grasshoppers speedily approach the comfort zone and swarm never come together towards the same point, the modified form GOA technique for solving optimization problems shown in equation-23 is

taken without considering gravity along with an assumption that wind is always tending to the target  $\hat{T}_d$ .

$$X_i^d = c \left( \sum_{l=1}^N c \frac{ub_d - lb_d}{2} S(|X_l^d - X_k^d|) \frac{X_l - X_k}{d_{kl}} \right) + \hat{T}_d \quad (23)$$

where  $ub_d$  and  $lb_d$  are upper bound and lower bound in  $D^{th}$  dimension,  $\hat{T}_d$  is value of the  $D^{th}$  dimension in the target, 'c' is a decreasing coefficient to shrink the comfort, attraction and repulsion zones. The parameters  $c$  counting for deceleration of grasshopper tending towards the food source and consuming it. Some random variables are multiplied both the terms in equation-22 for the counting of interaction of grasshopper. The mathematical formulations to explore and exploit the search space in addition to that of a search agent for tuning of exploration and exploitation level. In case of stochastic optimization, the first attention is to getting the promising regions in the search space in exploration stage and then the search agent is compelled by exploitation to find the global optimum value by searching locally. By increasing the no. of iterations which increases the behavior of grasshopper which can be influence by  $c$  value. The parameter 'c' requirement to be decreasing the proportion to the number of iterations in order to balance the exploration and exploitation. When 'c' decreases, the interactive forces among grasshoppers decrease. When 'c' increases in the search space about the target maxima value decreases. The declining coefficient  $c$  reducing the comfort zone is taken as

$$c = c_m - I \frac{c_m - c_n}{L} \quad (24)$$

Where  $c_m$  and  $c_n$  are max. and min. values of 'c' taken in the interval [1, 0.00001], I is the present iteration and L is represented maximum number of iterations in standard GOA technique, The converging characteristic in GOA is highly affected by the parameter 'c' in equation-24. With a lower value it results slow convergence towards the target. Therefore, the algorithm avoids getting stuck in relative optima which in turn increases the chance of getting global optima. In the proposed algorithm (iGOA), the value of 'c' decreases slowly at the starting and quickly during the end of

iteration from 1 to 0.00001 and the current iteration 'I' and maximum number of iterations, 'L' considered by a correction factor of 1.5 found by series of trial runs by which exploration of the algorithm increase. Thus equation-24 is modified as

$$c = c_m - I^{1.5} \left( \frac{c_m - c_n}{L^{1.5}} \right) \quad (25)$$

## 5. Simulation Result

### 5.1 SMIB Power System

The MATLAB/SIMULINK is used to create to develop model of the SMIB system which is shown in Fig.5. The current study used the variable step type ode23tb solver has been considered during simulation process of simulation model [4, 5]. MATLAB's Sim Power Systems library is used to design the model of the power system. The rotor reference frame(d-q) represents all winding dynamics. The subsystem of the SIMULINK block in the excitation system known as "Generator Control System" (Reg\_M) and the Hydraulic Turbine and Governor (HTG) system. The different researcher has attempted to iGOA optimization technique in different type of problem. It has been demonstrated that the improve Grasshopper Optimization Algorithm (GOA) [34,28] benefits from high exploration while exhibiting very fast convergence speed. Exploration and exploitation balance smoothly with the unique adaptive mechanism in this algorithm. These features possibly enable the GOA algorithm to deal with greater exploration of search space and outperform other methods. Furthermore, computational complexity is superior to that of many techniques, which is displayed in the literature. These powerful characteristics of the iGOA technique motivated us to propose this present study. In the proposed analysis initial part of analysis to demonstrated to shows that iGOA is least minimum ITAE value as compared to GOA, PSO and GA optimization in coordinated control of lead lag based SSSC controller of the system. For integral time absolute error (ITAE) calculations a 3-phase fault for 5 cycle is taken into account near the middle of one transmission line. In order to clear the fault, the

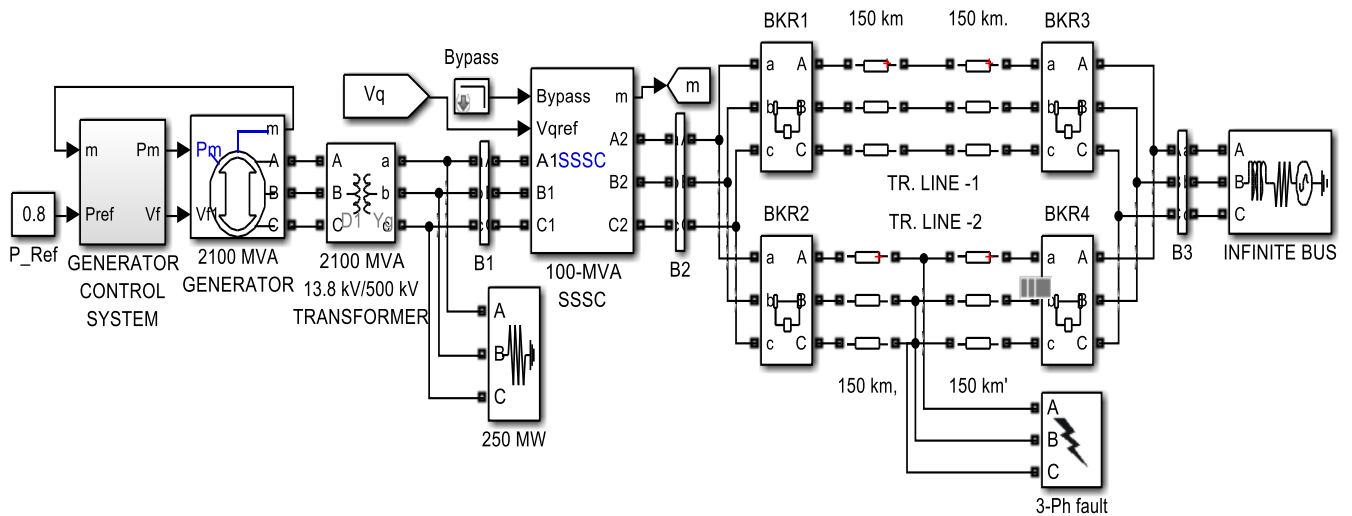


Fig. 5. MATLAB/SIMULINK model of SMIB system

lines are opened for five cycles. The PSS with LL based SSSC controller parameters are optimized by iGOA, GOA, PSO, and GA methods to demonstrate the better performance of the

iGOA approach. The 50 populations and 100 generations are taken in initial value of all the optimization algorithm during the optimization process of the system. All the optimization

algorithm are run minimum 30 times and the best optimal results (determined by the lowest ITAE value) are obtained controller's parameters. The Table 2 provided the optimal controller parameters of these techniques and its least ITAE value. From the Table 2, it is clear that, with a PSS with lead-lag controller of the power system which employed the iGOA technique is obtained the lowest ITAE values ( $5.0143 \times 10^{-4}$ ) as compared to GA ( $26.3557 \times 10^{-4}$ ), PSO ( $8.0246 \times 10^{-4}$ ), and GOA ( $7.8049 \times 10^{-4}$ ). Hence, from the Table-2, it is clear that iGOA based optimization design of coordinated control as compared to GA, PSO, and GOA techniques results in a reduction of the ITAE value of 80.97%, 37.51%, and 35.75% respectively in the same identical controller and same power system model. The proposed test model is demonstrated to observed that the superiority of iGOA over GA, PSO and GOA techniques. The system response of the dynamic behavior of speed deviation is shown in Fig.6. It is clear that the iGOA based controller is obtained the best system response performance as compared to GA, PSO, and GOA based PSS with LL based SSSC controller of the same power system. The next step of analysis of transient stability of same SMIB power system model Type-2 fuzzy PSS with T2FLL SSSC controller is implemented and which employed the iGOA technique to find out the optimal controller parameters. The tuning controller parameters for the iGOA technique are obtained as in Table 3 which is same same procedure as in previous analysis. It can be seen that the ITAE value  $3.8325 \times 10^{-4}$  further reduces in Type-2 fuzzy PSS with T2FLL controller as compared to the conventional PSS with LL controller of the same power system model. The J value is consequently 23.56% decreases with Type-2 fuzzy PSS with T2FLL than with the PSS with LL controller of the power system.

The effectiveness of Type-2 fuzzy PSS with T2FLL based SSSC controller is investigated under different cases of

loading condition and location of fault in the SMIB power system.

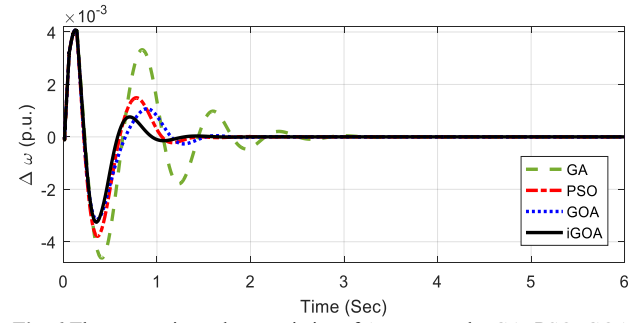


Fig. 6. The comparison characteristics of  $\Delta\omega$  among the GA, PSO, GOA and iGOA tuned Lead lag controller

Case-I: Severe disturbance Nominal loads ( $P_e=0.8$  p.u.  $\delta_0=48.50^\circ$ )

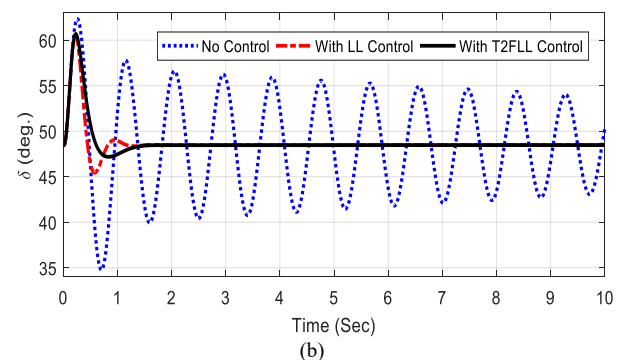
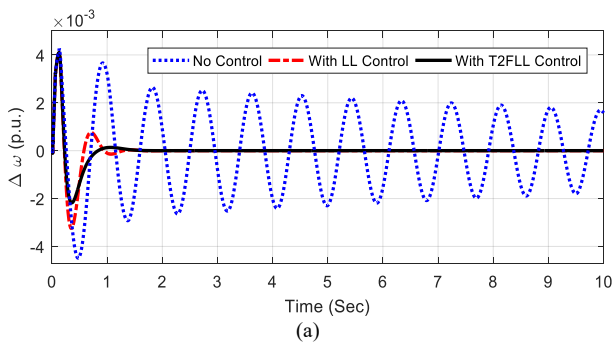
In Case-1 under nominal loading ( $P_e=0.8$  p.u.  $\delta_0=48.50$ ) is considered for initial testing process of the system. In the middle of one of the parallel lines, a 3-phase fault was imposed for 5 cycles. This disturbance is clear by opening the transmission line for five cycles. The different system responses of LL and T2FLL, both of which are tuned by iGOA, are shown in Figure 7(a)-(e). The legend 'No Control' is also shown in Figure 7(a)-(e) for comparison purposes. The deviation of rotor speed ( $\Delta\omega$ ) in per unit, power angle ( $\delta$ ) in degrees and the tie line real power ( $P_1$ ) in MW are shown in Figure 7(a)-(c) respectively. The output voltage of SSSC ( $V_q$ ) and PSS ( $V_s$ ) in p.u. are shown in Figure 7(d)-(e) respectively. It is demonstrated under the Case-1 of nominal loading condition of the synchronous generator with T2FLL based SSSC controller and compared to LL based SSSC damping controller of the same power system.

Table 2. Tuning parameters of PSS with LL based SSSC controller in SMIB

Strategy	Devices	K	T <sub>1</sub>	T <sub>2</sub>	T <sub>3</sub>	T <sub>4</sub>	J value x 10 <sup>-4</sup>
GA	SSSC	24.6047	0.4022	0.4359	0.6386	0.9258	26.3557
	PSS	22.5437	0.2833	0.6973	0.9579	0.9848	
PSO	SSSC	34.6061	0.7521	0.7639	0.7631	0.6199	8.0246
	PSS	11.2777	0.6793	0.9600	0.2976	0.2349	
GOA	SSSC	25.3571	0.6431	0.1992	0.6320	0.8249	7.8049
	PSS	20.7813	0.4482	0.2464	0.0410	0.5352	
iGOA	SSSC	64.7147	0.5838	0.7666	1.1562	0.9377	5.0143
	PSS	15.0296	0.2526	1.7872	1.3757	1.6760	

Table 3. iGOA tuned T2FLL based PSS with SSSC controller in SMIB

Controller/PSS	K <sub>SF1</sub>	K <sub>SF2</sub>	K	T <sub>1</sub>	T <sub>2</sub>	T <sub>3</sub>	T <sub>4</sub>	J value x 10 <sup>-4</sup>
SSSC controller	0.2008	0.0044	91.1917	1.8559	1.2631	0.6612	0.4737	3.8325
PSS	0.7972	0.0064	10.3531	0.0498	1.4952	0.0009	1.5993	



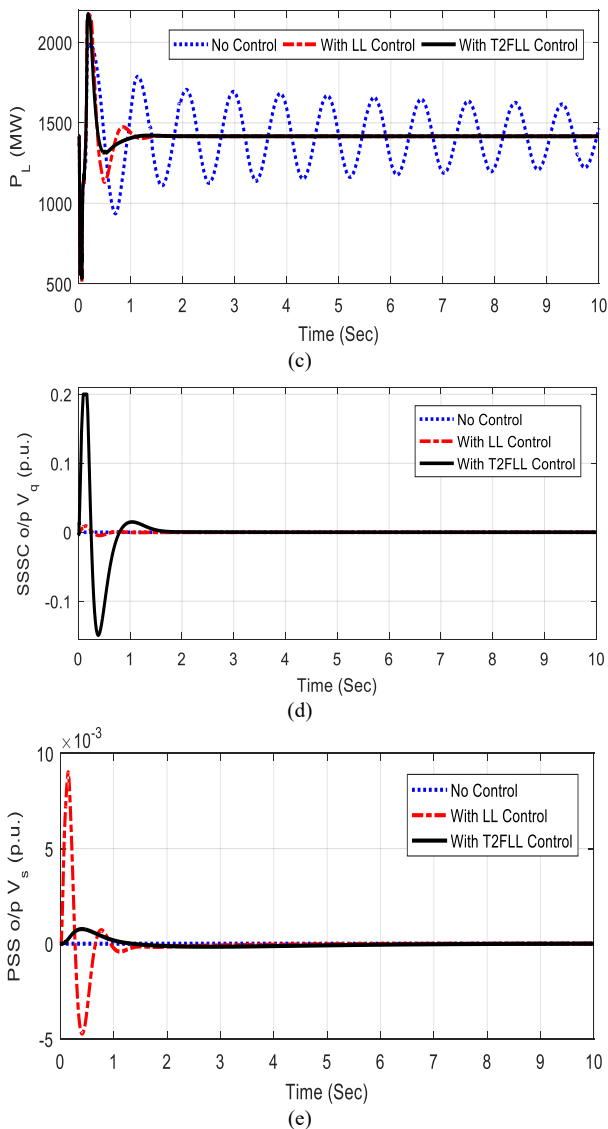


Fig. 7. System outcomes of SMIB for Case 1, (a)  $\Delta\omega$ , (b)  $\Delta\delta$ , (c)  $P_L$ , (d) SSSC output and (e) PSS output

It is clear from the Figures that suggested T2FLL based SSSC damping controller outperformed as compared to LL based SSSC controller in terms of damping capability in the same power system.

Case 2: Small Disturbance ( $P_e=1$  p.u.  $\delta_0=48.40$ )

In Case 2, the effectiveness of stability analysis of the power system can be tested in same T2LL controller under small disturbance conditions with heavy loading condition is considered. In this Case-2, the load is removed from bus 1 for 50 ms at  $t = 0$  sec of the proposed power system. The system responses for speed deviation, power angle and line active power are shown in Figure 8(a) to 8(c). The system responses shows that under no control the system is highly unstable. It is demonstrated under this condition and it is observed from the figures that the type-2 fuzzy PSS with T2FLL controller successfully suppressed the system oscillations under small disturbance condition of system. The proposed Type-2 fuzzy PSS with T2FLL based controller also offers a superior transient response as compared to PSS with LL based controller of the same system

Case 3: A new fault location and modified loading conditions ( $P_e=0.5$  p.u.,  $\delta_0 =38.20$ )

The effectiveness and robustness of the controller is further checked under various fault and loading condition. In Case-3, it is taken as light loading of the synchronous generator of the system and a 3-phase self-clearing fault is applied at bus 1 for 5 cycles. In this condition, the transient responses are obtained for  $\Delta\omega$  in p.u.,  $\delta$  in degree and  $P_L$  in MW which are as shown in Figure 9 (a)-(c). It is demonstrated under this Case-3 and it is observed from the demonstration that the damping of oscillation quickly damped out in Type-2 fuzzy PSS with T2FLL controller as compared to PSS with LL controller and no controller of the same power system. The improvement of transient stability performances for the three cases which are reflected in the Table-4. It is clear from the Table-4 that for different cases (Case-1, Case-2, Case-3) the Type-2 fuzzy PSS with T2FLL controller obtained least performances indexes as compared to PSS with LL and no controllers of the power system.

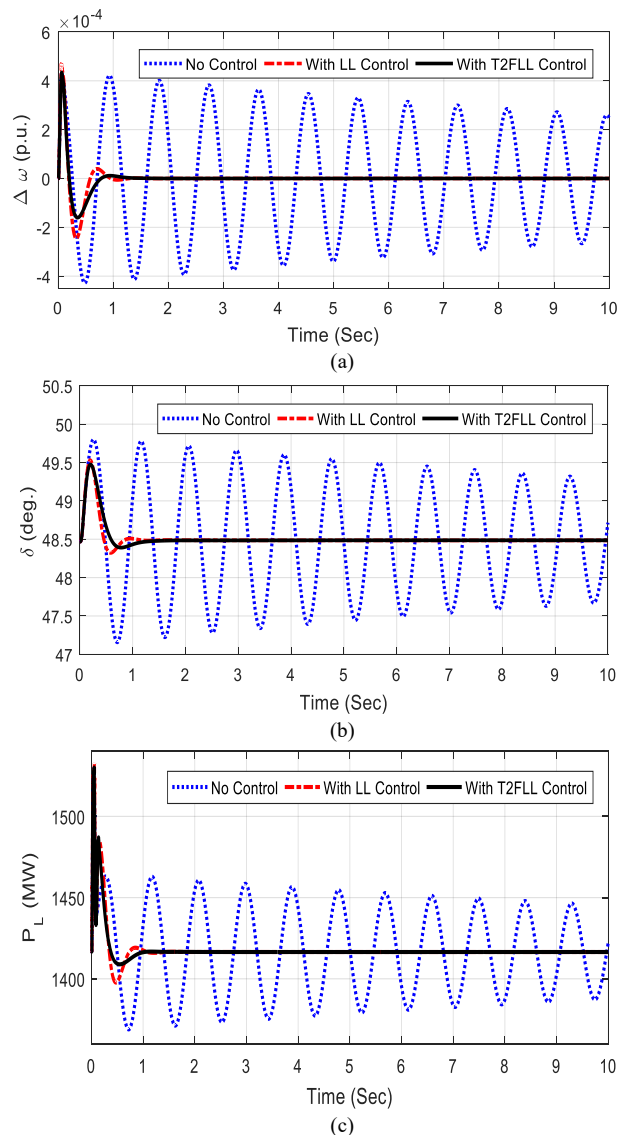


Fig. 8. Various outcomes of SMIB for Case 2 (a)  $\Delta\omega$ , (b)  $\Delta\delta$ , (c)  $P_L$

The improvement of transient performances in term of error of ISE, ITSE, ITAE, IAE and overshoots and undershoots in no control, LL and T2FLL controller of the same power system for the three cases which are reflected in the Table-4. It is clear from the Table-4 that for different cases (Case-1, Case-2, Case-3) that the Type-2 fuzzy PSS with T2FLL based SSSC damping controller obtained least

performances indexes as compared to LL based SSSC controller and no controllers of same the power system.

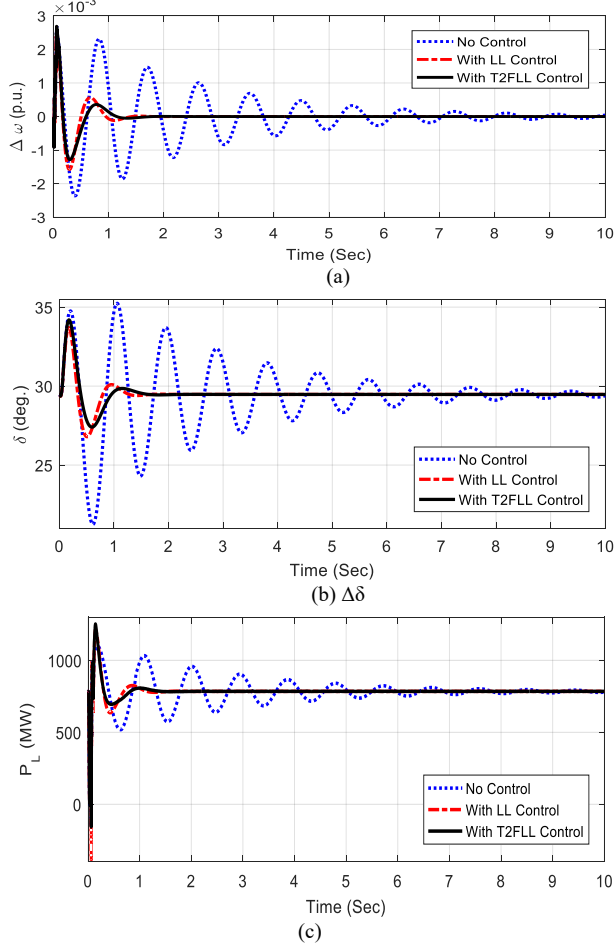


Fig. 9. Various outcomes of SMIB of Case 3, (a)  $\Delta\omega$ , (b)  $\Delta\delta$ , (c)  $P_L$

Table 4. Performance Indexing values under different cases in SMIB power system

Cases	Controller	ISE ( $\times 10^{-6}$ )	ITAE ( $\times 10^{-4}$ )	ITSE ( $\times 10^{-3}$ )	IAE ( $\times 10^{-6}$ )	Overshoots in $\Delta\omega$ ( $\times 10^{-3}$ )	Undershoots in $\Delta\omega$ ( $\times 10^{-3}$ )
Case 1	NC	32.2141	674.412	15.5684	114.9081	4.2709	-4.4916
	LL	3.6605	5.0143	1.4587	0.9287	4.0971	-3.2552
	T2FLL	2.8429	3.8325	1.2171	0.6082	4.0952	-2.3409
Case 2	NC	0.6001	100.0263	2.1803	2.5053	0.4346	-0.4286
	LL	0.0277	0.33401	0.1155	0.0053	0.4708	-0.2458
	T2FLL	0.0212	0.30437	0.1013	0.0037	0.4346	-0.1606
Case 3	NC	6.2824	126.3493	5.1473	9.3606	2.6901	-2.3547
	LL	0.8127	2.7305	0.7173	0.2001	2.5348	-1.5822
	T2FLL	0.7928	2.7011	0.7085	0.0177	2.6906	-1.3216

5.2 Extension to Multi Machine System (MMPS)

A MATLAB/SIMULINK environment is used to create the MMPS by taking the parameters as per the reference [33]. The simulation model of MMPS as shown in Fig.10. The detailed Fig.11 provides the specific simulation model of Area 1 and similar simulation model is developed for Area 2. The installation of FACTS devices in transmission line of power systems has significantly better in series FACTS controller. The sensitivity analysis may be used to choose the ideal position for SSSC in large power system depending on the goal that has to be achieved. To improve the stability of the power system, the SSSC is introduced in buses 1 and 2 as seen in MMPS. The suggested T2FLL controller is designed which employed similar method to that utilized in the SMIB scenario. The objective function for a system with multi machines system is defined by equation (14). The Tables 5 and 6 contain the optimized values for the PSS's with LL based SSSC controller and the PSS's with T2FLL based SSSC controller respectively

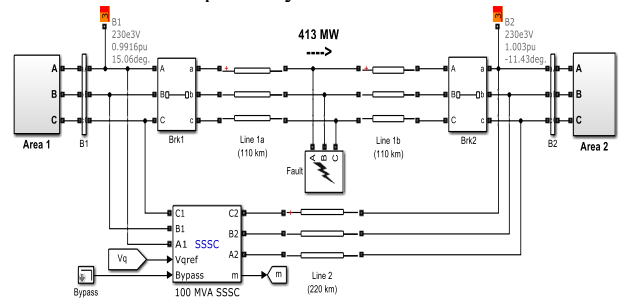


Fig. 10. The Multi-Machine two-area system developed by Kundur in SIMULINK

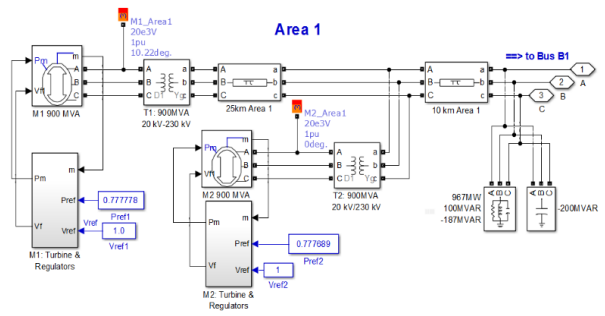


Fig. 11. SIMULINK model of area one of Kundur's multi-machine 4-area system

transmission lines suffers a self-clearing 3-phase fault for 5-cycle in the middle of line. The system is demonstrated under this condition and it observed that the Figure 12(a)-(b) shows that the local oscillations mode ( $\Delta\omega_{12}$ ) and inter area oscillations mode ( $\Delta\omega_{23}$ ) respectively of the proposed power system. It is observed from the Figure 12(a)-(b) that without control system is highly unstable the system and stability of the system is maintained both LL and T2FLL based SSSC damping controller of the power system. However, in Figure 12(a)-(b) shows that in Type-2 fuzzy PSS with T2FLL based SSSC controller the system improves damping performances in term of less overshoot and undershoots are obtained as compared to PSS with LL controller of the same power system

Case 1: Three-phase fault disturbance

The controller's performance is initially examined under large fault condition of the proposed multi machine power system. At time  $t=0$  seconds, it is considered that one of the parallel



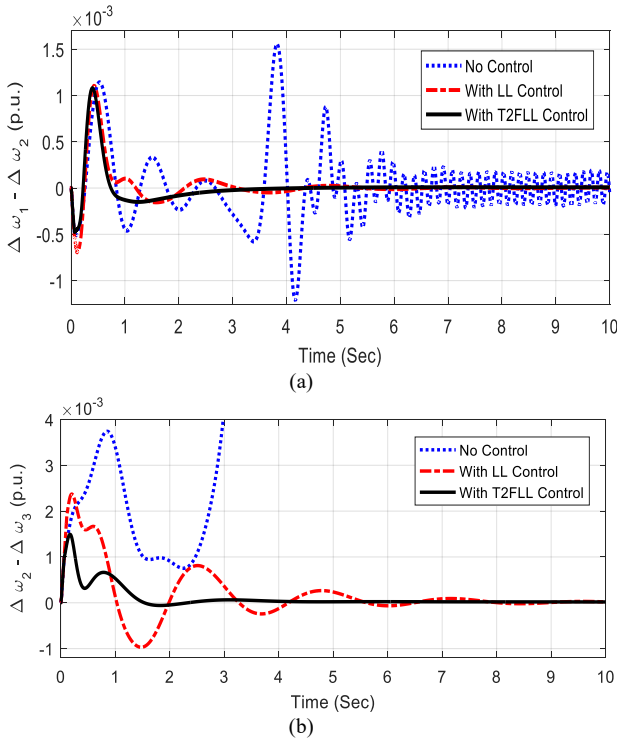


Fig. 12. (a) Case-1. Local oscillation mode of MMPS (b)Case-1 Interarea oscillation mode of MMPS.

Case 2: Disturbance due to a line outage

In the Case-2, one of the parallel lines is opened for at time t=0 sec. and closed again after 8 cycles of the power system. It is tested under this condition and found that system response of the local oscillation mode ( $\Delta\omega_{12}$ ) and interarea mode of oscillation ( $\Delta\omega_{23}$ ) of MMPS are depicted in Figure 13(a) and 13(b) respectively. From the Figure 13(a) and

13(b), it is clear that the system responses is highly unstable under no control and responses are obtained with Type-2 fuzzy PSS with T2FLL controllers gives better transient performances as compared to PSS with LL controllers of same system.

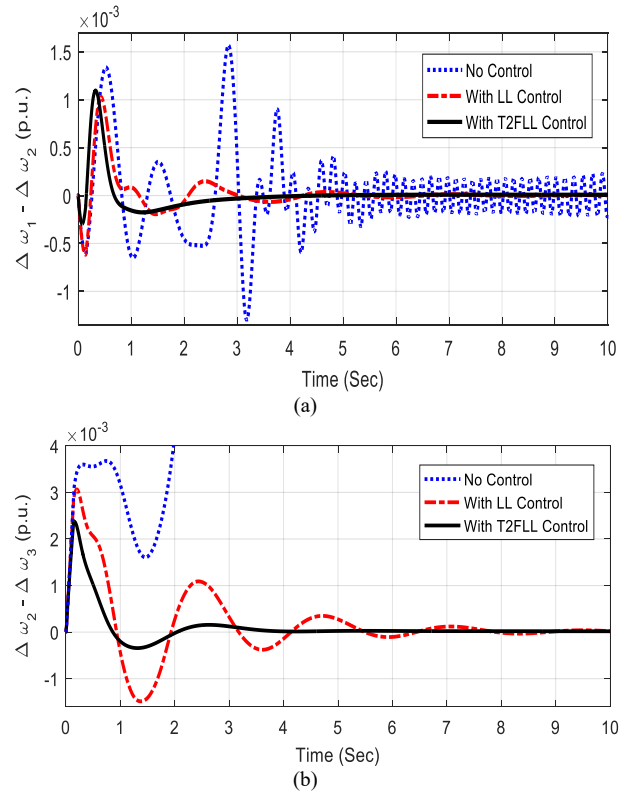


Fig. 13. (a). Case-II. Local oscillation mode of MMPS and (b). Case-II. Interarea oscillation mode of MMPS

Table 5. iGOA optimized constraints of PSS with LL based SSSC controller in MMPS.

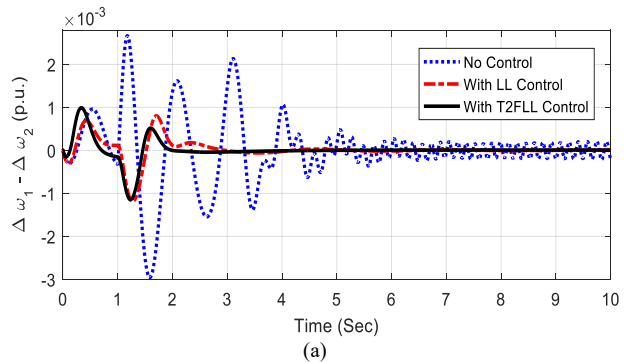
Controller/PSS	K	T <sub>1</sub>	T <sub>2</sub>	T <sub>3</sub>	T <sub>4</sub>
SSSC	80.5568	0.0240	0.0113	3.5894	2.7427
PSS1	22.8813	0.0833	0.0245	2.9337	3.4555
PSS2	19.6771	0.0769	0.0477	4.3201	4.1138
PSS3	23.8818	0.0354	0.0084	1.5122	2.4424
PSS4	23.7704	0.0501	0.0417	1.4203	4.7301

Table 6. The iGOA Optimized Constraints of T2FLL Based PSS and SSSC for MMPS.

Controller	K <sub>SF1</sub>	K <sub>SF2</sub>	K	T <sub>1</sub>	T <sub>2</sub>	T <sub>3</sub>	T <sub>4</sub>
SSSC	0.0084	0.0103	17.3554	0.0596	0.0022	1.3621	1.0884
PSS1	0.4353	0.0055	40.5297	0.0056	0.0018	1.4027	1.6215
PSS2	1.2772	0.0594	10.0684	0.0535	0.0037	1.2616	0.6086
PSS3	0.1186	0.0114	28.0181	0.0717	0.0057	0.9004	1.0935
PSS4	1.2809	0.1651	9.2040	0.0077	0.0026	1.3525	1.0942

Case 3: Small disturbance

In this case the reference voltage of machine-1(M1) is amplified by 5% for 12 cycle. The simulated results for the local mode of oscillation and the interarea mode of oscillation are shown in Figure 14(a) and 14 (b) respectively. The system responses are obtained in PSS with LL and Type-2 fuzzy PSS with T2FLL controllers both maintain a stable operation of the system. The Figure 14 however shows that response of Type-2 fuzzy PSS with T2FLL controller gives significantly better damping of low frequency oscillation as compared to the PSS with LL controller of the same system.



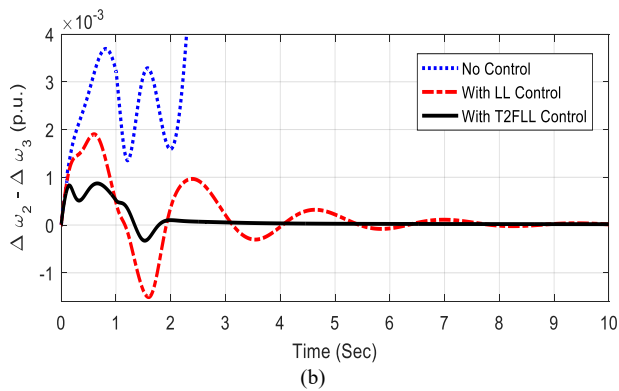


Fig. 14. (a) Case-3:Local oscillation mode of MMPS (b). Case-3: Interarea oscillation mode of MMPS

The Table 7 provides a summary of the outcomes of the optimal solution for MMPS in the above conditions are obtained. The Table-7 illustrates that the T2FLL controller consistently produces lower ITAE values than the LL controller under the three cases.

Table 7. ITAE value of T2FLL controller in MMPS under different Cases

Cases/ Controller	Case-1 ( $\times 10^{-3}$ )	Case-2 ( $\times 10^{-3}$ )	Case-3 ( $\times 10^{-3}$ )
NC	20349.8596	212460.9904	21041.0975
LL	33.5527	43.9984	39.1874
T2FLL	9.1413	11.1401	10.4856

## 6. Conclusion

In this analysis of proposed work, it is possible to improve the system's stability by using a Type-2 fuzzy PSS with T2FLL

based SSSC damping controller. An improved grass hopper algorithm (iGOA) approach is used to tune the coordinate control of PSS and LL based SSSC controller of the SMIB system. The design superiority of iGOA optimised based PSS with LL controller over GOA, PSO, and GA optimized control of the same power system is first proved. It is found that iGOA reduces the ITAE value in PSS with LL controllers by 80.97%, 37.51%, and 35.75%, respectively as compared to GA, PSO, and GOA optimized same controller with same SMIB power system. In the second part of analysis, the design of a Type-2 fuzzy PSS with T2FLL based SSSC controller is applied to SMIB power system. It is obtained that ITAE value reduced by 23.56% as compared to conventional PSS with LL controller of the same system. It is demonstrated under different loading and location of fault of the power system. It is observed that enhancement of the damping of the system shows better in Type-2 fuzzy PSS with T2FLL controller as compared to PSS with LL controller of the same the system. Finally, the effectiveness and robustness of the proposed damping controller is investigated in case of MMPS for transient stability enhancement. The comparison between various responses under different disturbance scenarios have been considered in MMPS. The demonstration of power system models observed that the Type-2 fuzzy PSS with T2FLL based SSSC damping controller perform superior damping control as compared to conventional PSS with LL based SSSC damping controller for power system stability improvement.

This is an Open Access article distributed under the terms of the Creative Commons Attribution License.



## References

- [1] Y. Yu, *Electric Power System Dynamics*. New York: Academic Pr, 1983.
- [2] P. W. Sauer, M. A. Pai, and J. H. Chow, *Power System Dynamics and Stability: With Synchrophasor Measurement and Power System Toolbox 2e: With Synchrophasor Measurement and Power System Toolbox*, 1st ed. Wiley, 2017. doi: 10.1002/9781119355755.
- [3] L. Gyugyi, C. D. Schauder, and K. K. Sen, "Static synchronous series compensator: a solid-state approach to the series compensation of transmission lines," *IEEE Trans. Power Delivery*, vol. 12, no. 1, pp. 406–417, Jan. 1997, doi: 10.1109/61.568265.
- [4] M. A. Abido and Y. L. Abdel-Magid, "Robust design of multimachine power system stabilisers using tabu search algorithm," *IEE Proc., Gener. Transm. Distrib.*, vol. 147, no. 6, p. 387, 2000, doi: 10.1049/ip-gtd:20000717.
- [5] Y. L. Abdel-Magid, M. A. Abido, S. Al-Baiyat, and A. H. Mantawy, "Simultaneous stabilization of multimachine power systems via genetic algorithms," *IEEE Trans. Power Syst.*, vol. 14, no. 4, pp. 1428–1439, Nov. 1999, doi: 10.1109/59.801907.
- [6] K. Sebaa and M. Boudour, "Optimal locations and tuning of robust power system stabilizer using genetic algorithms," *Elect. Pow. Syst. Res.* vol. 79, no. 2, pp. 406–416, Feb. 2009, doi: 10.1016/j.epr.2008.08.005.
- [7] S. Paul and P. K. Roy, "Oppositional cuckoo optimization algorithm for optimal tuning of power system stabilizers," in *Michael Faraday IET International Summit 2015*, Kolkata, India: Institution of Engineering and Technology, 2015, p. 30 (6.)-30 (6.). doi: 10.1049/cp.2015.1626.
- [8] M. A. Abido, "Robust design of multimachine power system stabilizers using simulated annealing," *IEEE Trans. On energy Conversion*, vol. 15, no. 3, pp. 297–304, Sep. 2000, doi: 10.1109/60.875496.
- [9] S. Mishra, M. Tripathy, and J. Nanda, "Multi-machine power system stabilizer design by rule based bacteria foraging," *Elec. Pow. Syst. Res.*, vol. 77, no. 12, pp. 1595–1607, Oct. 2007, doi: 10.1016/j.epr.2006.11.006.
- [10] S. Panda, N. K. Yegireddy, and S. K. Mohapatra, "Hybrid BFOA–PSO approach for coordinated design of PSS and SSSC-based controller considering time delays," *Int. J. of Elect. Pow. & Ener. Sys.*, vol. 49, pp. 221–233, Jul. 2013, doi: 10.1016/j.ijepes.2013.01.006.
- [11] R. Kumar, R. Singh, and H. Ashfaq, "Stability enhancement of multi-machine power systems using Ant colony optimization-based static Synchronous Compensator," *Comp. & Elect. Eng.*, vol. 83, p. 106589, May 2020, doi: 10.1016/j.compeleceng.2020.106589.
- [12] R. K. Khadanga and S. Panda, "A Modified Local Input Signal for SSSC-Based Damping Controller Design," *Elect. Pow. Comp. and Sys.*, vol. 49, no. 11–12, pp. 978–989, Jul. 2021, doi: 10.1080/15325008.2021.1985016.
- [13] B. Vijay Kumar, G. Rajendar, and V. Ramaiah, "Optimal location and capacity of Unified Power Flow Controller based on chaotic krill herd blended runner root algorithm for dynamic stability improvement in power system," *Int. J. Num. Model.*, vol. 34, no. 2, p. e2828, Mar. 2021, doi: 10.1002/jnm.2828.
- [14] R. K. Khadanga and S. Panda, "A Modified Local Input Signal for SSSC-Based Damping Controller Design," *Elect. Pow. Comp. and Sys.*, vol. 49, no. 11–12, pp. 978–989, Jul. 2021, doi: 10.1080/15325008.2021.1985016.
- [15] E. K. Bindumol, V. Mini, and N. Chandran, "Coordinated Control of PSS and SSSC using PSO to Improve Power System Stability,"

- in *Emerging Technologies for Sustainability*, 1st ed., P. C. Thomas, V. J. Mathai, and G. Titus, Eds., CRC Press, 2020, pp. 293–302. doi: 10.1201/9780429353628-38.
- [16] M. A. Kamarposhti, I. Colak, C. Iwendi, S. S. Band, and E. Ibeke, “Optimal Coordination of PSS and SSSC Controllers in Power System Using Ant Colony Optimization Algorithm,” *J. Circ. Sys. Comp.*, vol. 31, no. 04, p. 2250060, Mar. 2022, doi: 10.1142/S0218126622500608.
- [17] E. V. Fortes, L. F. B. Martins, M. V. S. Costa, L. Carvalho, L. H. Macedo, and R. Romero, “Mayfly Optimization Algorithm Applied to the Design of PSS and SSSC-POD Controllers for Damping Low-Frequency Oscillations in Power Systems,” *Int. Trans. Electr. Ener. Sys.*, vol. 2022, pp. 1–23, Apr. 2022, doi: 10.1155/2022/5612334.
- [18] P. R. Sahu, P. K. Hota, S. Panda, R. K. Lenka, S. Padmanaban, and F. Blaabjerg, “Coordinated Design of FACTS Controller with PSS for Stability Enhancement Using a Novel Hybrid Whale Optimization Algorithm – Nelder Mead Approach,” *Elec. Pow. Comp. Sys.*, vol. 49, no. 16–17, pp. 1363–1378, Oct. 2021, doi: 10.1080/15325008.2022.2129860.
- [19] J. Ansari, A. R. Abbasi, M. H. Heydari, and Z. Avazzadeh, “Simultaneous design of fuzzy PSS and fuzzy STATCOM controllers for power system stability enhancement,” *Alexandria Eng. J.*, vol. 61, no. 4, pp. 2841–2850, Apr. 2022, doi: 10.1016/j.aej.2021.08.007.
- [20] P. R. Sahu, R. K. Lenka, R. K. Khadanga, P. K. Hota, S. Panda, and T. S. Ustun, “Power System Stability Improvement of FACTS Controller and PSS Design: A Time-Delay Approach,” *Sustainability*, vol. 14, no. 21, p. 14649, Nov. 2022, doi: 10.3390/su142114649.
- [21] S. Dadfar, K. Wakil, M. Khaksar, A. Rezvani, M. R. Miveh, and M. Gandomkar, “Enhanced control strategies for a hybrid battery/photovoltaic system using FGS-PID in grid-connected mode,” *Int. J. Hydr. Ener.*, vol. 44, no. 29, pp. 14642–14660, Jun. 2019, doi: 10.1016/j.ijhydene.2019.04.174.
- [22] V. P. Rajderkar and V. K. Chandrakar, “Design Coordination of a Fuzzy-based Unified Power Flow Controller with Hybrid Energy Storage for Enriching Power System Dynamics,” *Eng. Technol. Appl. Sci. Res.*, vol. 13, no. 1, pp. 10027–10032, Feb. 2023, doi: 10.48084/etasr.5508.
- [23] A. Rezvani, A. Esmacily, H. Etaati, and M. Mohammadinodoushan, “Intelligent hybrid power generation system using new hybrid fuzzy-neural for photovoltaic system and RBFNSM for wind turbine in the grid connected mode,” *Front. Energy*, vol. 13, no. 1, pp. 131–148, Mar. 2019, doi: 10.1007/s11708-017-0446-x.
- [24] P. K. Ray *et al.*, “A Hybrid Firefly-Swarm Optimized Fractional Order Interval Type-2 Fuzzy PID-PSS for Transient Stability Improvement,” *IEEE Trans. on Ind. Applicat.*, vol. 55, no. 6, pp. 6486–6498, Nov. 2019, doi: 10.1109/TIA.2019.2938473.
- [25] S. R. Paital, P. K. Ray, and S. R. Mohanty, “A robust dual interval type-2 fuzzy lead-lag based UPFC for stability enhancement using Harris Hawks Optimization,” *ISA Transact.*, vol. 123, pp. 425–442, Apr. 2022, doi: 10.1016/j.isatra.2021.05.029.
- [26] P. R. Sahu, P. K. Hota, S. Panda, H. V. Long, and T. Allahviranloo, “Modified grasshopper optimization algorithm optimized adaptive fuzzy lead-lag controller for coordinated design of FACTS controller with PSS,” *IFS*, vol. 43, no. 4, pp. 5075–5094, Aug. 2022, doi: 10.3233/JIFS-212716.
- [27] S. Saremi, S. Mirjalili, and A. Lewis, “Grasshopper Optimisation Algorithm: Theory and application,” *Adv. Engin. Softw.*, vol. 105, pp. 30–47, Mar. 2017, doi: 10.1016/j.advengsoft.2017.01.004.
- [28] P. M. Dash, S. K. Mohapatra, and A. K. Baliarsingh, “Automatic generation control of power systems with unified power flow controller by improved grasshopper optimization algorithm,” in *2020 International Conference on Computational Intelligence for Smart Power System and Sustainable Energy (CISPSSSE)*, Keonjhar, India: IEEE, Jul. 2020, pp. 1–6. doi: 10.1109/CISPSSSE49931.2020.9212264.
- [29] A. Zakeri and A. Hokmabadi, “Efficient feature selection method using real-valued grasshopper optimization algorithm,” *Exp. Sys. with Applic.*, vol. 119, pp. 61–72, Apr. 2019, doi: 10.1016/j.eswa.2018.10.021.
- [30] A. L. Bukar, C. W. Tan, and K. Y. Lau, “Optimal sizing of an autonomous photovoltaic/wind/battery/diesel generator microgrid using grasshopper optimization algorithm,” *Solar Energy*, vol. 188, pp. 685–696, Aug. 2019, doi: 10.1016/j.solener.2019.06.050.
- [31] S. Arora and P. Anand, “Chaotic grasshopper optimization algorithm for global optimization,” *Neural Comput & Applic.*, vol. 31, no. 8, pp. 4385–4405, Aug. 2019, doi: 10.1007/s00521-018-3343-2.
- [32] L. Abualigah and A. Diabat, “A comprehensive survey of the Grasshopper optimization algorithm: results, variants, and applications,” *Neural Comput & Applic.*, vol. 32, no. 19, pp. 15533–15556, Oct. 2020, doi: 10.1007/s00521-020-04789-8.
- [33] P. S. Kundur and O. P. Malik, *Power system stability and control*, Second edition. New York Chicago San Francisco Athens London Madrid Mexico City Milan New Delhi Singapore Sydney Toronto: McGraw Hill, 2022.
- [34] A. K. Patra and S. K. Mohapatra, “Coordinated control of PI type PSS and MISO PI type SSSC-based damping controller design using improved grasshopper optimisation algorithm,” *IJCSE*, vol. 25, no. 4, p. 421, 2022, doi: 10.1504/IJCSE.2022.124565.
- [35] S. K. Mohapatra and S. Panda, “Stability enhancement with SSSC-based controller design in presence of non-linear voltage-dependent load,” *IJISTA*, vol. 15, no. 2, p. 163, 2016, doi: 10.1504/IJISTA.2016.076499.